

Mapping the Hidden Universe: The Universe Behind the Milky Way – The Universe in HI
ASP Conference Series, Vol. 3 $\times 10^8$, 2000
R. C. Kraan-Korteweg, P. A. Henning, and H. Andernach, eds.

IR-TF Relation in the Zone of Avoidance with 2MASS

Nicolas Bouché, Stephen Schneider

*University of Massachusetts, Department of Astronomy, Lederle
Graduate Tower, Amherst, MA 01003, USA*

Abstract. Using the Tully-Fisher (TF) relation, one can map the peculiar velocity field and estimate the mass in regions such as the Great Attractor. The Two Micron All Sky Survey (2MASS) is surveying the full sky in J, H and K bands and has the great advantage that it allows us to detect galaxies more uniformly to lower Galactic latitude than optical surveys. This study shows the feasibility of using 2MASS and the TF relation to probe large-scale structure. We found that (i) we can use axial ratio b/a up to 0.5; (ii) intrinsic extinction is present (up to 0.5 mag at J, 0.1 mag at K); (iii) the zero-point of the TF relation is independent of the 2MASS magnitude measurement; (iv) the 2MASS K-band 20th mag/arcsec² isophotal aperture magnitude produces the best TF relation; and (v) there is no type dependence of the residuals.

1. Introduction. The Tully-Fisher Relation

In 1977, Tully and Fisher discovered that there is a good correlation between maximum rotational velocity, usually given by the global neutral hydrogen line profile width ΔV (corrected for inclination) and the absolute magnitude M for late-type galaxies (Tully & Fisher 1977).

Observationally, the correlation (luminosity vs. maximum velocity) gives $L \propto \Delta V^\alpha$ with α in the range of 2.5-3 at optical wavelengths. There is a general trend that at longer wavelengths, the slope steepens. At infrared wavelengths, the slope ($-2.5 \times \alpha$ in magnitudes) climbs to about -10 (or $\alpha \sim 4$) which is close enough to the Faber-Jackson relation $L \propto \sigma_v^4$ to suspect a possible common physical origin.

The origin of the TF relation lies (in the very roughest terms) in the virial theorem. Assuming a constant mass-to-light ratio (M/L) and constant surface brightness (I), one can rewrite the virial theorem as

$$L \propto V^4 [(M/L)^2 I]^{-1} \quad (1)$$

The zero-point is directly related to basic physical properties as can be seen if rewritten as $-2.5 \times \log[I(M/L)^2]$ or $\log[(M/L)\Sigma]$. Σ is the surface mass density which is a strong function of the angular momentum ($\Sigma \propto M^7/J^4$) whereas the mass-to-light ratio gives information on the stellar content. This can be used to put strong constraints on galaxy formation theory (see Steinmetz & Navarro 1999; Koda et al. 2000).

Zwaan et al. 1995 also have shown that low surface brightness late-type galaxies follow the same B-band TF relation as the high surface brightness galaxies, even though their mass-to-light ratios are very different as well as the ratio of dark to luminous matter (de Blok & McGaugh 1997), but this is still somewhat controversial (see O'Neil et al. 2000).

The HST Key Project group on the extragalactic distance scale has used the TF relation to infer the Hubble constant (H_0) (see Sakai et al. 2000 for a recent discussion). Another application is to use the TF relation to measure the peculiar velocity field of galaxies. This provides an estimate of the mass density on large scales and of the density of the universe through $\Omega^{0.6}/b$.

Using near-IR for TF studies has two advantages: (1) it is sensitive to old red stars and less sensitive to young blue stars. In other words, it is fairly independent of current star formation, so it provides a measure of current stellar content that is, presumably, more closely tied to the total mass of the galaxy and hence its kinematics; (2) uncertainties due to interstellar absorption in both our own Galaxy and in the observed galaxy are greatly reduced.

This project shows the feasibility of using 2MASS (Huchra et al. these proceedings; Jarrett et al. 2000) and HI data to study large scale structure. We studied the Pisces-Perseus (PP) supercluster region and the Great Attractor (GA) region in the Zone of Avoidance. In particular, we ask the following questions regarding 2MASS:

- (i) Which band (J, H or K) generates the best TF relation?
- (ii) What magnitude measurement gives the tightest TF relation?
- (iii) Can we use 2MASS data at low Galactic latitude?

and regarding the TF relation:

- (iv) What is the highest axial ratio b/a that we can use?
- (v) Is there any internal extinction?

The remainder of this paper is organized as follows. In section 2, we present our data sets. The method is described in section 3. Our results are presented in section 4 and summarized in section 5.

2. Data Sets

We construct two data sets. The first (PP) data set consists of HI data selected from the Huchtmeier & Richter catalog (Huchtmeier & Richter 1989). Because we found substantial scatter was introduced when using line widths measured in different ways, we select only papers with Giovanelli and collaborators. The data was also restricted to the Arecibo telescope and measurements made at 50% of the peak. The sample contains ~ 2700 objects. We cross-matched 2MASS data with the Giovanelli subsample. There were 502 matches as of spring 1999¹. This sample covers the sky from 0^h to 5^h in right ascension and 15° to 35° in declination which corresponds to the Pisces-Perseus supercluster region.

We also used HI data from Giovanelli et al. 1997 from their extensive survey of the I-band TF in clusters. We again cross-matched this subsample with the

¹As of January 2000, there are about 3 times as many matches, but the analysis is not completed.

2MASS database and obtained 300 matches from 22 different clusters (hereafter *cluster* sample). We took into account the different offsets from the Hubble flow (column (4) in Table 2 of Giovanelli et al. 1997) for each cluster. This sample also contains inclination information both from I-band photometry and from 2MASS which enabled us to perform checks on the 2MASS estimate of the axial ratio.

3. Method and Error Budget

3.1. Sub-Sample

In most cases, we used a subsample of galaxies chosen to have the following properties: (i) axial ratio b/a less than 0.5 (the axial ratio used was the “super coadd” axial ratio, keyword *sup_ba* in the 2MASS database, which is determined from the coadded J, H and K images); (ii) H I flux minimum of 1 Jy km s⁻¹ in order to remove low SNR H I data; (iii) magnitude cutoff of K=13 mag (in the PP sample, we had a cutoff on the magnitude errors ($\sigma = 0.1$) which corresponds to a cutoff in magnitude of ~ 13 determined from the dependence of the magnitude errors with magnitude); (iv) excluding S0’s and ellipticals (in general, the b/a constraint and H I detection are sufficient to ensure that no ellipticals are in the subsample), and (v) redshifts between z_{min} and z_{max} to examine galaxies in different distance ranges.

Figure 1 shows the TF relation for the *cluster* sample.

3.2. Corrections

In order to improve the quality of the TF relation, a number of corrections are usually made for turbulent motion, instrumental broadening, and extinction. These corrections have a number of adjustable parameters that we investigate here to determine which values or methods work best with the 2MASS data.

We have corrected for (i) instrumental broadening following Bottinelli et al. (1990) and Giovanelli et al. (1997); (ii) turbulent motion according to the scheme proposed by Tully & Fouqué 1985 (this correction is small and did not improve the scatter of the TF relation); (iii) inclination, i.e. $v_{rot} = \frac{W_R}{2 \sin i}$ where W_R is the observed velocity width W_{50} corrected for instrumental broadening and i is the disk inclination based on the axial ratio b/a from 2MASS, and (iv) photometric corrections such as the Galactic extinction (from COBE/ DIRBE maps, Schlegel et al. 1998) and internal extinction $\Delta m = -\gamma \log b/a$ where γ characterizes the extinction for a highly inclined galaxy. In general, γ can be a function of galaxy luminosity or velocity width (see Sakai et al. 2000 and references therein), but we treated it as a constant.

3.3. Parameterization and Error Budget

We parameterize the TF relation in the same way as Giovanelli et al. (1997), $y = a + bx$ where y is the absolute magnitude and x is the logarithm of the rotation velocity, i.e.:

$$x = \log \left[\frac{W_R}{2 \sin i} \right] - 2.5 \quad (2)$$

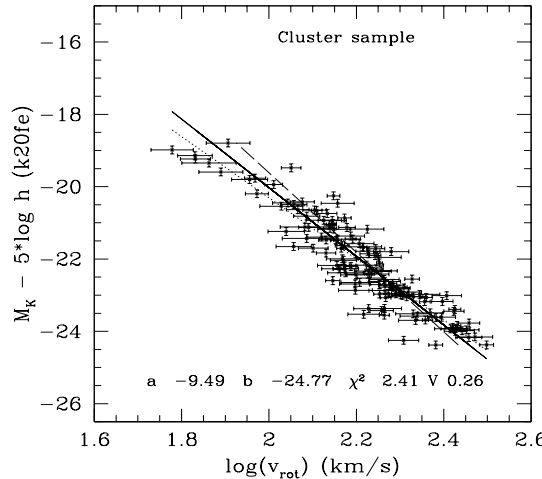


Figure 1. TF relation for a sub-sample (130 objects) of the *cluster* data set with axial ratio $b/a < 0.5$, H I flux > 1 Jy km s $^{-1}$, magnitude $m_K < 13$. The slope, a , and zero-point, b , are shown as well as the χ^2_{min} and the variance V . The dotted line is a direct fit, the dashed line is an inverse fit and the bivariate fit is the solid line with an intrinsic scatter σ_i of 0.2 mag. No internal extinction correction was made here.

$$\begin{aligned}
 y &= (m_{obs} - A - \Delta m - k_z - 5 \log \frac{cz}{100h_{100}} - 25) - 5 \log h_{100} \\
 &= M - 5 \log h_{100}
 \end{aligned} \tag{3}$$

where h_{100} is the Hubble constant in units of 100 km s $^{-1}$ Mpc $^{-1}$. The last term $-5 \log h_{100}$ makes y independent of the Hubble constant so it is easier to compare results with other authors. k_z is the k -correction and was generally ignored here since the sample contains only nearby galaxies ($cz < 10,000$ km s $^{-1}$).

A standard χ^2 fit to the data was performed using errors both along the x and y axes, σ_x and σ_y (*bivariate fit*). σ_x includes velocity width uncertainty as well as inclination errors, which dominate the overall error. σ_y includes magnitude uncertainty from 2MASS, distance uncertainty, and an added intrinsic scatter σ_i which takes into account any “cosmological” scatter inherent in the TF relation. The 1σ uncertainty on the parameters (a and b) is given by the projection of the 1σ contour semi-major axis onto the parameter axis (Press et al. 1992).

4. Results and Discussion

2MASS produces many different magnitude measurements for each object (Jarrett et al. 2000). The different types of magnitude that we used are (i) the 20th

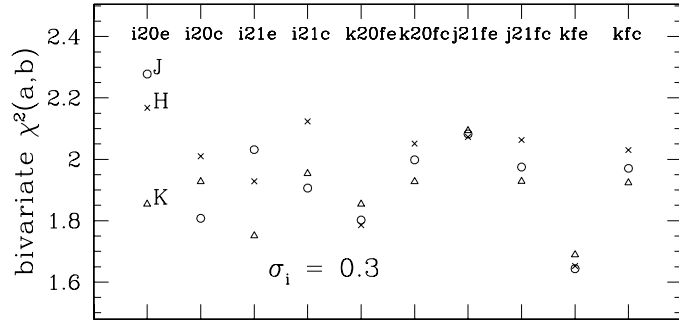


Figure 2. For each of the magnitude types, the reduced χ^2 value of the fit is shown, where the circles are for the J-band magnitude, the crosses are for the H-band, and the triangles are for the K-band. Circular (elliptical) aperture magnitudes are indicated the suffix *c* (*e*). This is for the *cluster* data set using 2MASS axial ratios for the inclination and an intrinsic scatter σ_i of 0.3 mag.

mag/arcsec² isophotal magnitude (*i20* in the 2MASS database ²); (ii) the 21st mag/arcsec² isophotal magnitude (*i21*); (iii) the 20th mag/arcsec² K fiducial ³ magnitude (*k20f*); (iv) the 21st mag/arcsec² J fiducial magnitude (*j21f*), and (v) the Kron (Kron 1980) K fiducial (*kf*) magnitude which measures the flux within an aperture $2r_1$ where r_1 is the first moment of the light distribution. This type of magnitude is thought to be less sensitive to observing conditions and is thought to be a “total” measure of the integrated flux (Koo 1986).

First, which band J, H or K produces the least scatter in the TF relation? Figure 2 shows the minimum value χ^2_{min} of the bivariate fit for each of the magnitude types. Figure 2 indicates that (1) the *20th mag/arcsec² K fiducial magnitude* and Kron K fiducial produces the smallest scatter; (2) in general K gives a tighter TF relation than J or H, considering that H-band photometry of 2MASS is subject to uncertainty due to air glow; and (3) elliptical apertures tend to give a better TF relation than circular ones, although this was not consistently true for all datasets.

Since the different magnitude types have different measurement errors, the χ^2_{min} could look artificially low if the error estimates were inflated. However, we found no effects of this sort. Magnitude types with the largest mean measurement error did not produce the smallest χ^2 .

² In order to find the proper keyword in the 2MASS database, one needs to add the prefix *j-m-*, *h-m-* or *k-m-* and the suffix *e* (*c*) for elliptical (circular) aperture.

³2MASS has two kinds of magnitude type, “individual” (*i20* and *j21* here) and “fiducial” (*k20f*, *j21f* and *kf* here). “Fiducial” means the aperture used for the photometry was selected at one band and applied to the other two.

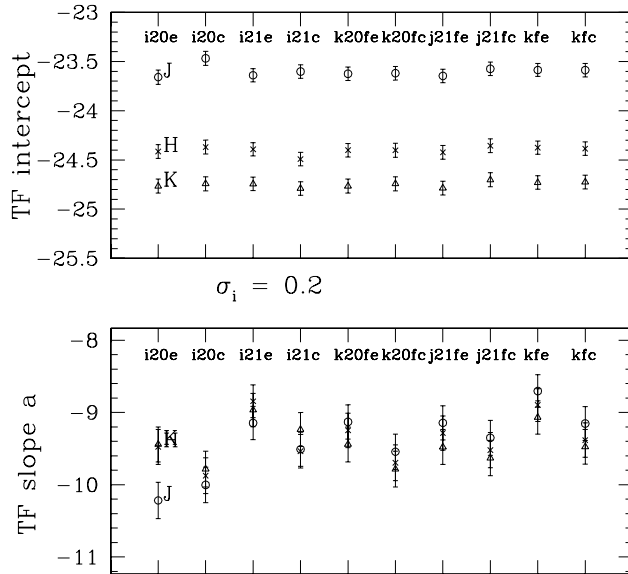


Figure 3. Top panel: Intercept of the TF fit for each of the magnitude types. For each of the magnitudes, the circles are for the J-band magnitude, the crosses are for the H-band, and the triangles are for the K-band. Circular (elliptical) aperture magnitudes are indicated by the suffix *c* (*e*). Notice that the zero points are all within $1-\sigma$ of each other especially at K. Bottom panel: Slopes of the TF relation for each of the magnitude types. Both panels are for the *cluster* sub-sample using 2MASS axial ratios with no internal extinction correction.

Figure 3 shows the fitted values of the slope, a , and the zero-point, b , for each of the magnitude types assuming an intrinsic scatter σ_i of 0.2 for the *cluster* sub-sample and using the 2MASS axial ratios for the inclination. First note that the zero-point of the TF relation is well determined and does not depend on the magnitude used. Second, the slope is more dependent on the magnitude type. However, the “fiducial” magnitudes are well within $1-\sigma$ of each other. Third, the slope tends to be steeper as the wavelength increases. This is often called the color-TF relation. The same conclusions can be reached using either the 2MASS or I-band inclinations and different values of σ_i .

Figure 4 shows the value of the reduced χ^2 as a function of γ for the PP sample using the magnitude $k20fc$ and an intrinsic scatter of 0.2 mag. We find a minimum for each band: ~ 0.5 mag at J, ~ 0.3 at H and ~ 0.1 at K, although the amount of extinction at K is consistent with none. These curves are consistent with our results from the *cluster* sample, however, they are not fully reproduced when using the inclination from the I-band photometry. Our results are consistent with a reddening of $E(B-V)$ of 0.5 mag which gives a A_λ of 0.45 mag, 0.28 and 0.18 for the three bands.

We did not see any correlation with type for the *cluster* data set while the PP data set shows a slight correlation. A linear fit gives a non-zero slope (-0.06) with $1-\sigma$ uncertainty of 0.03 for the PP data set, such that both results are consistent with no type dependence (at the 95% confidence level).

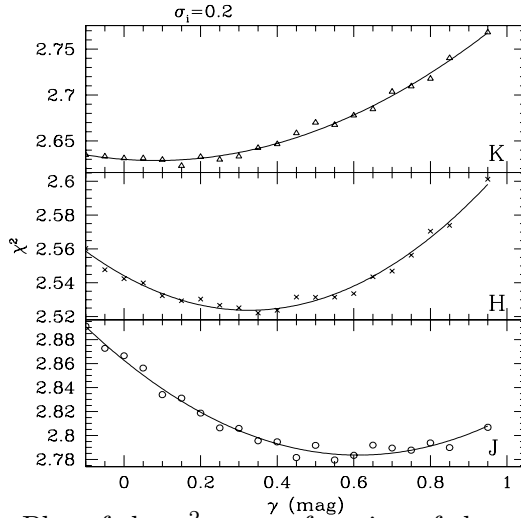


Figure 4. Plot of the χ^2_{min} as a function of the parameter γ for the PP data set. The panels correspond to J, H and K starting from the bottom. The open symbols are the data points while the solid line is a fit of a second order polynomial. The amount of extinction (at the minimum of each curve) decreases as the wavelength increases as one would expect.

We have not tested for dependence of the TF relation on surface brightness because the current 2MASS galaxy processor is not very sensitive to low surface brightness disks. Attempts are underway to extract them in the future.

5. Conclusions

From our two samples (PP and *cluster* data sets), we found that using K-band is generally preferable over the other bands. The K-fiducial 20th mag/arcsec² (and the K-fiducial Kron, although in the PP sample, the Kron K-fiducial does not produce such a low χ^2) seems to produce the least scatter. This is consistent with the K-fiducial isophotal elliptical aperture magnitude being the most robust photometric measurement (Jarrett et al. 2000). At low Galactic latitude, preliminary results suggests one would need optical axial ratios because the high star density can mislead the 2MASS ellipse-fitting program. The zero-point is well determined and is even independent of the magnitude types and of the sample. The TF slope shows more scatter but it steepens with wavelength. An interesting result is that we find internal extinction at each band, although the amount of extinction at K is consistent with none. We find no type dependence in our samples but we cannot yet conclude whether there is a surface brightness dependence.

Our results are summarized below for the PP sample (equations 4 & 5) and the *cluster* sample (equations 6 & 7) using an intrinsic scatter of $\sigma_i = 0.2$ and assuming $\gamma = 0.1$ mag of internal extinction.

$$M_K - 5 \log h_{100} = (-9.90 \pm 0.35) \cdot (\log v_{rot} - 2.5) + (-24.70 \pm 0.10) \quad (4)$$

$$M_K - 5 \log h_{100} = (-9.64 \pm 0.35) \cdot (\log v_{rot} - 2.5) + (-24.76 \pm 0.09) \quad (5)$$

$$M_K - 5 \log h_{100} = (-9.63 \pm 0.27) \cdot (\log v_{rot} - 2.5) + (-24.74 \pm 0.08) \quad (6)$$

$$M_K - 5 \log h_{100} = (-9.58 \pm 0.29) \cdot (\log v_{rot} - 2.5) + (-24.86 \pm 0.10) \quad (7)$$

Equations 4 & 6 are for the $k20fc$ magnitude, while equations 5 & 7 are for the $k20fe$ magnitude. Both samples give very similar results.

As part of future work to study large scale flows in the ZOA, we have recently collected H I data at Arecibo for low Galactic latitude galaxies. Of 169 sources at $|b| < 10^\circ$, 72 were detected; of 147 sources at $10^\circ < |b| < 20^\circ$, 75 were detected. The galaxies were identified using the 2MASS galaxy processor, which holds promise for identifying a large sample of galaxies within the ZOA.

Acknowledgments N. Bouché is the recipient of a Five College Astronomy Graduate Fellowship supported by the Mary Dailey Irvine Fund which allowed him to attend the meeting.

References

Bottinelli, L., Gouguenheim, L., Fouqué, P., & Paturel, G. 1990, A&AS, 82, 391
 de Blok, W.J.G., & McGaugh, S.S. 1997, MNRAS, 290, 533
 Giovanelli, R., Haynes, M.P., Herter, T., & Vogt, N. 1997, AJ, 113, 53
 Huchtmeier, W.K., & Richter, O.G. 1989, A&A, 210, 1
 Jarrett, T.H., Chester, T., Cutri, R., Schneider, S., Skrutskie, M., & Huchra, J.P. 2000, AJ, 119, 2498
 Koda, J., Sofue, Y., & Wada, K. 2000, ApJ, 531, L17
 Koo, D.C. 1986, ApJ, 311, 651
 Kron, R.G. 1980, ApJS, 43, 305
 O'Neil, K., Bothun, G.D., & Schombert, J. 2000, AJ, 119, 1360
 Press, W.H., Teukolsky, S.A., Vetterling, W.T., & Flannery, B. 1992, Numerical Recipes in C, (Cambridge: Cambridge University Press)
 Sakai, S., Mould, J.R., Hughes, S.M.G., et al. 2000, ApJ, 529, 698
 Schlegel, D.J., Finkbeiner, D.P., & Davis, M. 1998, ApJ, 500, 525
 Steinmetz, M., & Navarro, J.F. 1999, ApJ, 513, 555
 Tully, B., & Fisher, R. 1977, A&A, 54, 661
 Tully, B., & Fouqué, P. 1985, ApJS, 58, 67
 Zwaan, M.A., van der Hulst, J.M., de Blok, W.J.G., & McGaugh, S.S. 1995, MNRAS, 273, L35